Tellus (2000), 52B, 348–374
Printed in UK. All rights reserved

TELLUS
ISSN 0280–6509

Observations of the evolution of the aerosol, cloud and boundary-layer characteristics during the 1st ACE-2 Lagrangian experiment

By DOUG W. JOHNSON[1]*, SIMON OSBORNE[1], ROBERT WOOD[1], KARSTEN SUHRE[2], PATRICIA K. QUINN[3], TIM BATES[3], M. O. ANDREAE[4], KEVIN J. NOONE[5], PAUL GLANTZ[5], BRIAN BANDY[6], J. RUDOLPH[7] and COLIN O'DOWD[8], [1]*Met. Research Flight, Building Y46, DERA, Farnborough, Hants, UK;* [2]*University of Toulouse, France;* [3]*PMEL, NOAA, Seattle, USA;* [4]*MPIC, Mainz, Germany;* [5]*MISU, University of Stockholm, Sweden;* [6]*University of East Anglia, UK;* [7]*University of York, Canada;* [8]*CMAS, University of Sunderland, UK*

(Manuscript received 21 April 1999; in final form 22 September 1999)

ABSTRACT

During the 1st Lagrangian experiment of the North Atlantic Regional Aerosol Characterisation Experiment (ACE-2), a parcel of air was tagged by releasing a smart, constant level balloon into it from the Research Vessel *Vodyanitskiy*. The Meteorological Research Flight's C-130 aircraft then followed this parcel over a period of 30 h characterising the marine boundary layer (MBL), the cloud and the physical and chemical aerosol evolution. The air mass had originated over the northern North Atlantic and thus was clean and had low aerosol concentrations. At the beginning of the experiment the MBL was over 1500 m deep and made up of a surface mixed layer (SML) underlying a layer containing cloud beneath a subsidence inversion. Subsidence in the free troposphere caused the depth of the MBL to almost halve during the experiment and, after 26 h, the MBL became well mixed throughout its whole depth. Salt particle mass in the MBL increased as the surface wind speed increased from 8 m s^{-1} to 16 m s^{-1} and the accumulation mode (0.1 μm to 3.0 μm) aerosol concentrations quadrupled from 50 cm^{-3} to 200 cm^{-3}. However, at the same time the total condensation nuclei (>3 nm) decreased from over 1000 cm^{-3} to 750 cm^{-3}. The changes in the accumulation mode aerosol concentrations had a significant effect on the observed cloud microphysics. Observational evidence suggests that the important processes in controlling the Aitken mode concentration which, dominated the total CN concentration, included, scavenging of interstitial aerosol by cloud droplets, enhanced coagulation of Aitken mode aerosol and accumulation mode aerosol due to the increased sea salt aerosol surface area, and dilution of the MBL by free tropospheric air.

1. Introduction

For global climate models to accurately assess the direct and indirect forcing of aerosols they must include the physical and chemical processes that modify and age the atmosphere's natural and anthropogenically produced aerosols and their precursors. These processes have to be parameterized in terms of the bulk parameters of these models as they act on time and length scales much shorter than the model time steps or model grid boxes. Therefore, a thorough knowledge and understanding of these processes is required. Process models (Van Dingenen et al., 1999; Fitzgerald, 1998) and chemical transport models

* Corresponding author: Meteorological Research Flight, Building Y46, DERA, Farnborough, Hants, GU14 0LX, UK.
e-mail: dwjohnson@meto.gov.uk

(Taylor and Penner, 1994) continue to make progress with this but to further reduce the model uncertainties it is essential that more detailed experimental data sets are produced. In particular, in order to understand aerosol processing it is important that measurements are made in a Lagrangian framework as a process can only be identified by measuring the rate of change of a given parameter within an air parcel as a function of time.

The Atlantic Stratocumulus Transition Experiment (ASTEX, Albrecht et al., 1995; Huebert et al., 1996) and the 1st Aerosol Characterisation Experiment (ACE-1, Bates et al., 1998) have shown that effective large scale, Lagrangian experiments can be carried out and useful information about the processing of aerosols in the lower troposphere can be obtained (Clarke et al., 1998). During June and July 1997 a further field program, ACE-2 (Raes et al., 2000), was undertaken in the sub-tropical North Atlantic to characterise the aerosol and atmospheric chemistry there and to understand the processes effecting the evolution of the aerosol advected over the North Atlantic. As part of this project, a series of Lagrangian experiments (Johnson et al., 2000) were carried out. The purpose of this paper is to describe the measurements taken in the 1st Lagrangian experiment, which investigated the MBL, aerosol, chemistry and cloud microphysical evolution in a clean maritime air mass.

Understanding the origin of condensation nuclei (CN) in the remote marine environment has been the subject of many investigations (Bates et al., 1998). They are derived from a number of different sources, such as:

(a) marine biota. Dimethylsulphide (DMS) emitted from the ocean surface is probably the most important natural source of sulphur based aerosols (Andreae and Crutzen, 1997; Chin and Jacob, 1996) through the conversion to SO_2 in the MBL which can nucleate new aerosol or condense on to existing aerosol surface area;

(b) sea salt aerosol produced by surface wind stress under relatively high wind conditions causing breaking waves, which result in air bubbles bursting and producing water film and jet drops that can evaporate leaving a salt particle residual (Blanchard and Woodcock, 1957; O'Dowd and Smith, 1993; O'Dowd et al., 1997). This can then be mixed up to higher altitudes in the MBL through turbulent eddies;

(c) entrainment of aerosol from the free troposphere. The long life time of precursor gases in the upper troposphere can nucleate new aerosol particles that subside down to the top of the MBL and are entrained into it and continually top up the aerosol in the MBL (Raes, 1995; Clarke et al., 1998).

Once in the MBL the aerosol characteristics can further be modified by processes such as cloud processing, which tends to increase the size of the accumulation mode aerosol particles by aqueous phase chemistry (Dore et al., 2000) and reduce the accumulation mode concentration by droplet coalescence (Fiengold et al., 1996). Phoretic effects associated with the cloud droplets can also cause in cloud scavenging of interstitial aerosol, which will reduce aerosol concentrations and increase the size of the particles. Also, out of cloud, coagulation of aerosol and wet and dry deposition to the surface can reduce total aerosol concentrations.

The experiment reported on here identifies the important processes acting in a clean environment in a rapidly changing MBL. Sections 2 and 3 give a description of the data set and origin of the air mass. The thermodynamic and dynamic evolution of the MBL are described in Section 4 and the evolution of the aerosol and cloud microphysics is given in Sections 5 and 6. In Section 7 the chemical characteristics of the aerosol and trace gases are given. Section 8 summarises the conclusions and suggests hypotheses of the important processes in this experiment that can be tested in future work by detailed process models.

2. Measurements and data sets

Between 3 and 5 July 1997 the 1st ACE-2 Lagrangian experiment was undertaken. Two measurement platforms were involved: the Research Vessel (R/V) *Vodyanitskiy*, and the Meteorological Research Flight (MRF) C-130 aircraft. From 2035z until 2330z on 3 July at a position of 39.94°N, 10.92°W, just off the Portuguese coast, the R/V *Vodyanitskiy* released a plume of Perfluorocarbon (PFC) gas into the MBL followed by a smart balloon (Johnson and Businger, 2000) just after midnight on 4 July 1997 at 40.23°N, 11.20°W. Then, while the ship followed

Table 1. *A summary of the start and end times and positions of the MRF C-130 aircraft during the 3 flights it undertook during the 1st Lagrangian experiment; the numbers in brackets refer to the MRF aircraft flight numbers*

Flight	Start time (GMT)	End time (GMT)	Start position	End position
1st flight (A551)	00:16 4/7/97	03:35 4/7/97	40.5°N 11.5°W	39.9°N 11.3°W
2nd flight (A552)	11:39 4/7/97	16:56 4/7/97	37.7°N 10.9°W	36.3°N 11.3°W
3rd flight (A553)	22:25 4/7/97	02:35 5/7/97	34.0°N 12.3°W	32.2°N 13.1°W

the balloon along the first part of its trajectory, to measure the initial air parcel aerosol and trace gas characteristics and the DMS surface fluxes, the MRF C-130 aircraft carried out 3 consecutive back-to-back flights. Although this required a complete change of aircrew and scientists on each flight, it enabled the parcel to be sampled as continuously as possible with just one aircraft for almost 30 h. Table 1 shows the time and measurement positions of the MRF C-130 during the 3 flights. Johnson et al. (2000) give a plot of the flight pattern used during this experiment. The smart balloon released from the ship was set up to stay at around 600 m altitude, which was estimated to be the mid-height of the MBL. It did well at staying at that altitude and no adjustment to it was required during the flights.

Full details of the instruments used on board the platforms are given in Johnson et al. (2000), Bates et al. (2000) and Quinn et al. (2000). Further information about the resolution and accuracy of the aircraft instrumentation can be found in Rogers et al. (1995). Only brief details of the instruments used for the analysis presented in this paper will be given here. The physical aerosol characteristics in the MBL and lower free troposphere were determined using a Particle Measuring System's (PMS) passive cavity aerosol spectrometer probe (PCASP) mounted externally on the aircraft (Martin et al., 1995). This sized and counted particles in the accumulation mode (0.1 μm to 3.0 μm diameter) in 15 size bins and was operated with its de-icing heaters switched off so that the aerosol was sampled in near ambient RH conditions. Total condensation nuclei ($CN > 3$ nm) were measured using a TSI 3025 particle counter mounted inside the aircraft and sampled through a near isokinetic inlet. In addition, a counterflow virtual impactor (CVI, Noone et al., 1988) connected to a TSI 3010 particle counter and a PCASP, was used in 2 modes. In cloud it measured cloud drop residuals from cloud drops larger than 3 μm, while out of cloud it was used in aerosol mode to count and size particles larger than 10 nm. In both modes the aerosol was collected on filters so that it could be chemically characterised using ion chromotography. Other filter samples were collected through 2 aerosol, isokinetic sampling inlets at ambient RH. Further details of this and the analysis techniques used can be found in Andreae et al. (1988), and Talbot et al. (1990).

Cloud microphysical measurements were made using an externally mounted PMS forward scattering spectrometer probe (FSSP) which sizes and counts cloud droplet diameters between 2 μm and 47 μm (Martin et al., 1995). Liquid water contents (LWC) in cloud were measured with a Johnson–Williams liquid water probe (Baumgardner, 1983) and total water contents (TWC) determined using a lyman-α hygrometer (Nicholls et al., 1990).

The flight pattern carried out by the MRF C-130 aircraft was designed to characterise the physical and chemical properties of the aerosol in the air parcel being followed, and to establish the structure of the MBL at the same time. An initial profile was flown into the area of the balloon and, based on the measured thermodynamic structure of the MBL, a series of box patterns at altitudes best suited for sampling the different layers in the MBL and lower free troposphere were undertaken. The box patterns drifted with the wind and were positioned approximately 10 km behind the balloon. The closed box patterns were also used (Sollazzo et al., 2000) to calculate the divergence in the lower free troposphere and MBL to determine entrainment rates between the different layers in the lower atmosphere. Entrainment rates were also obtained using an eddy correlation technique on the measurements made on each of the straight

and level runs of the box patterns. All of the measurements presented in this paper can be found in the ACE-2 data archive at the Joint Research Center in Ispra, Italy.

3. Origin of air mass

At mid-day on 4 July 1997, a large anticyclone was positioned just to the north of the Azores and significant ridging to the west of Ireland was occurring behind a weakening cold front. Thus the wind off the coast of Portugal was from the northwest but became more north easterly over the Canary Islands. Verver et al. (2000) show a more detailed analysis of the synoptic situation during this experiment. Three-dimensional back trajectories calculated from NCEP analyses (Draxler and Hess, 1997 — HYSPLIT4 program), and shown in Johnson et al. (2000), indicate that the air originated over the centre of the North Atlantic and did not pass over land in the previous 5 days. Thus, the air was relatively clean and maritime in origin. The trajectories also indicate there was significant subsidence (0.45 cm s^{-1} on average) occurring in the free troposphere. Fig. 1 shows a METEOSAT satellite picture of the area with the back trajectories superimposed on it. Most of the trajectories shown end at the top of the MBL as the balloon passes underneath it and the star indicates the position of the balloon at the time of the satellite picture. The area to the north effected by the anticyclone was covered with a layer of stratocumulus. However, in the south-eastern part of the anticyclone the cloud was broken and convective in appearance and off the coast of southwest Portugal the skies were cloud-free.

4. Thermodynamic and dynamic evolution of the MBL

Due to the relatively large subsidence rates occurring in the free troposphere, the height of the MBL changed considerably during the experiment. The depth of the MBL decreased from over 1500 m at the start of the experiment, to less than 900 m at the end. Fig. 2 shows selected profiles from the three MRF C-130 flights which details the change in structure of the MBL and lower

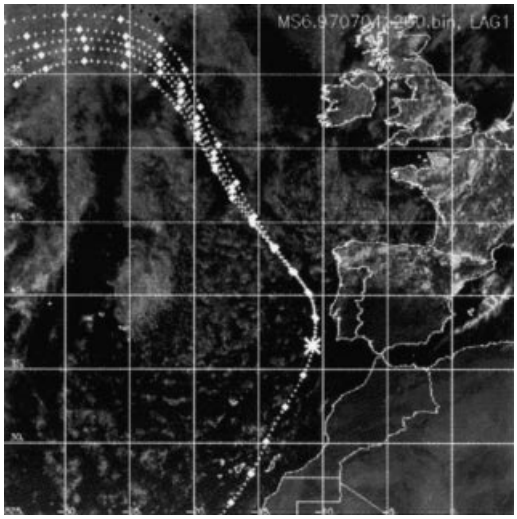

Fig. 1. A METEOSAT visible satellite picture for the ACE-2 area for mid-day on 4 July 1997 during the 1st Lagrangian experiment. Superimposed on the picture are air parcel model back trajectories starting at the top of the boundary layer as the balloon passes under it. The star indicates the position of the balloon at the time of the picture. The dotted trajectory, which passes over the Canary Islands is a model trajectory of the air at the altitude of the balloon in the SML. A more detailed explanation and description of these trajectories can be found in Johnson et al. (2000).

free troposphere throughout the experiment. Initially, the MBL was relatively deep and multi-layered, and capped by a 3 K temperature inversion underneath which was a well-broken layer of stratocumulus. There was a moist, shallow, surface mixed layer (SML) that extended up to 500 m. Above it there was a second mixed layer (CL — cloud layer) which was capped by the cloud and separated from the SML by a shallow stable transition region (TR). Well scattered cumulus clouds were observed to grow from the top of the SML, which was conditionally unstable, and some extended up to the subsidence inversion where they flattened out into the stratocumulus cloud layer that was mostly likely formed by the spreading out of the cumuli. These features can best be seen in the profile of equivalent potential temperature (θ_e) for the 1st flight shown in Fig. 2. The 2 well-mixed layers are characterised by constant values of θ_e; 315 K in the SML and 309 K in the CL. The broken nature of the cloud can also be clearly seen in Fig. 1.

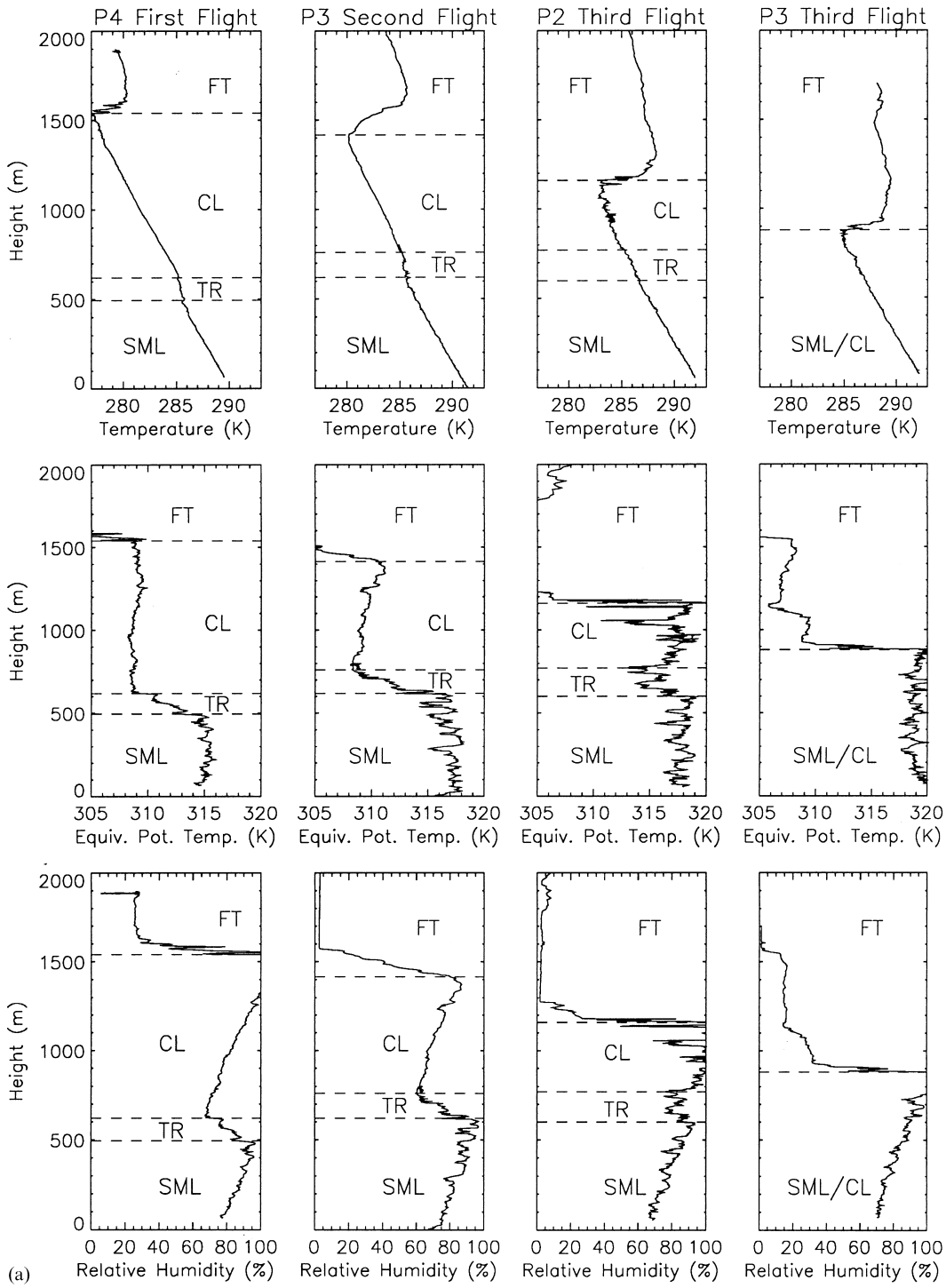
P4 First Flight
P3 Second Flight
P2 Third Flight
P3 Third Flight
Height (m)
2000
1500
1000
500
0
FT
CL
TR
SML
SML/CL
280 285 290
Temperature (K)
305 310 315 320
Equiv. Pot. Temp. (K)
0 20 40 60 80 100
Relative Humidity (%)

(a)

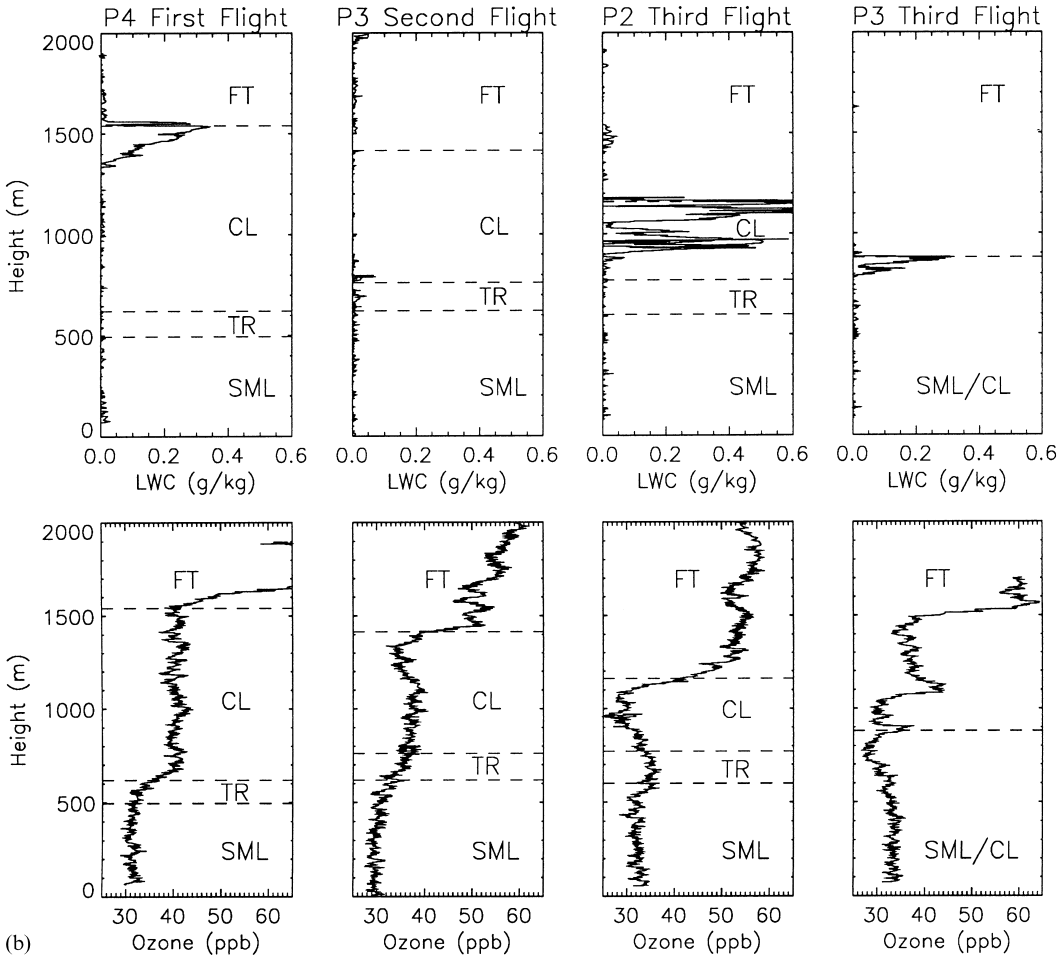

Fig. 2 (cont'd).

During the last 2 flights, the height of the inversion progressively decreased and strengthened to between 5 K and 6 K. In profile P3 of the 2nd flight (Fig. 2) no cloud was encountered under the subsidence inversion. Here the inversion is deeper with a smaller temperature gradient. The TWC in the CL is around 6.5 g/kg, which is much lower than that found in the SML that starts at approximately 9.1 g/kg and slowly rises with time to approximately 9.5 g/kg. In the SML, and CL the RH is observed to linearly increase with height with almost a step change in the TR. The surface

Fig. 2. (a) MRF C-130 aircraft profiles from the 3 flights in the 1st Lagrangian experiment. The first column shows profile P4 (0254 GMT 4 July 1997) from the 1st flight, the second column profile P3 (1453 GMT 4 July 1997) from the 2nd flight, and the third and fourth columns profile P2 (2225 GMT on 4 July 1997) and P3 (02:13 GMT 5 July 1997) respectively from the 3rd flight. The first row shows temperature, the second equivalent potential temperature, the third relative humidity. The horizontal dashed lines indicate the top and bottom of the layers observed in the boundary layer, i.e., the surface mixed layer (SML), the cloud layer (CL), the transition region between the SML and the CL (TR), and the free troposphere (FT). (b) Same as (a) except the first row shows liquid water content and the second row ozone concentration.

RH is generally around 70% but at the time of the balloon release, the ship reported the RH to be 83%.

In contrast to the MBL, the SML deepens during the 3 flights. At the beginning of the experiment, the SML has a depth of 500 m but as the experiment progresses it gets deeper until during the 3rd flight it is observed to merge with the subsidence inversion at 900 m. This accords with the measurements of cloud penetrations and observations from the flight deck, which showed that on the 1st flight, the cumulus clouds encountered had a large vertical extent and some of them were flattening out into stratocumulus underneath the inversion. On the 2nd flight, during the middle of the day on 4 July, the cumulus clouds were small and well scattered, though on the 3rd flight, on the night of the 4/5 July, more clouds were encountered but their vertical extent was limited and the cumuli were more prone to flattening out into stratocumulus, until in the very final profile of the experiment only shallow, broken stratocumulus was seen. This is borne out in Fig. 2 that shows LWC profiles. In half the profiles (not all are shown in Fig. 2), the aircraft did not pass through any cloud. The LWC profile during P4 of the 1st flight and P3 of the 3rd flight is characteristic of a stratocumulus sheet, whereas the other cloud penetrations look more like you would expect to see when passing through cumuli underlying stratocumulus as can be seen in profile P2 of the 3rd flight.

To show how the structure of the MBL evolved in a more continuous fashion, the measurements made in all the aircraft profiles, have been interpolated onto a grid so that vertical-time cross-sections can be constructed. This is shown in Fig. 3 for θ_e. The analysis has necessitated some data smoothing so that the fine detail has been lost but the overall large scale changes remain. The sharp change in height of the base of the subsidence inversion from 1500 m to 900 m during the experiment can be seen, and as the subsidence continues in the free troposphere the inversion at the top of the MBL strengthens. It also shows well the stable region between the SML and the well-mixed CL and the SML depth increasing with time. The increase in depth of the SML is probably due to a combination of 2 things:

(a) An increase in the surface wind speed that generated increased turbulent kinetic energy and enhanced mixing in the SML.

(b) An increase in the sea surface temperature (SST) along the length of the balloons trajectory which increased surface heat fluxes.

Fig. 4 shows aircraft profiles of wind speed and direction during the experiment. Again, the layered structure of the MBL can be identified. In the SML, the wind speed and direction is constant in the vertical but it increases significantly with time, from 8 m s^{-1} to 16 m s^{-1}, and the direction veers from 330° to 030°. These are all in agreement with the trajectory of the balloon, which was in the SML, except near the start of the 1st flight where it was probably in the TR between the SML and the CL (see Johnson and Businger, 2000). Generally, the wind speed was higher in the CL compared to the SML and there was often vertical wind shear through the TR, the CL and the subsidence inversion.

The SST was determined using the aircraft Heimann KT remote radiometer at the lowest point in each of its profiles and in the lowest box patterns. The variation of SST is shown in Fig. 5, with the ECMWF analysed SST which agree to within 0.5 K. It can be seen that the SST increases from 292 K to almost 295 K. This in combination with the surface water vapour flux helps to raise the SML θ_e from 315 K to 319 K.

A schematic diagram summarising the evolution of the MBL structure and cloud characteristics throughout the 1st Lagrangian experiment is shown in Fig. 6. This is based on evidence from all the profiles and box patterns carried out by the aircraft, and on the manually recorded observations made by the aircraft scientists during the flights.

5. Evolution of aerosol in the MBL

Not surprisingly, considering the changes in the thermodynamic and dynamic structure of the MBL during the experiment, some dramatic changes were observed in the aerosol characteristics. The most startling change was a quadrupling of the number concentration of accumulation mode (0.1 μm to 3.0 μm diameter) aerosol particles in the MBL. Fig. 7 shows profiles of the accumulation mode concentration (N) and mean volume diameter. In the 1st flight, the SML was clean

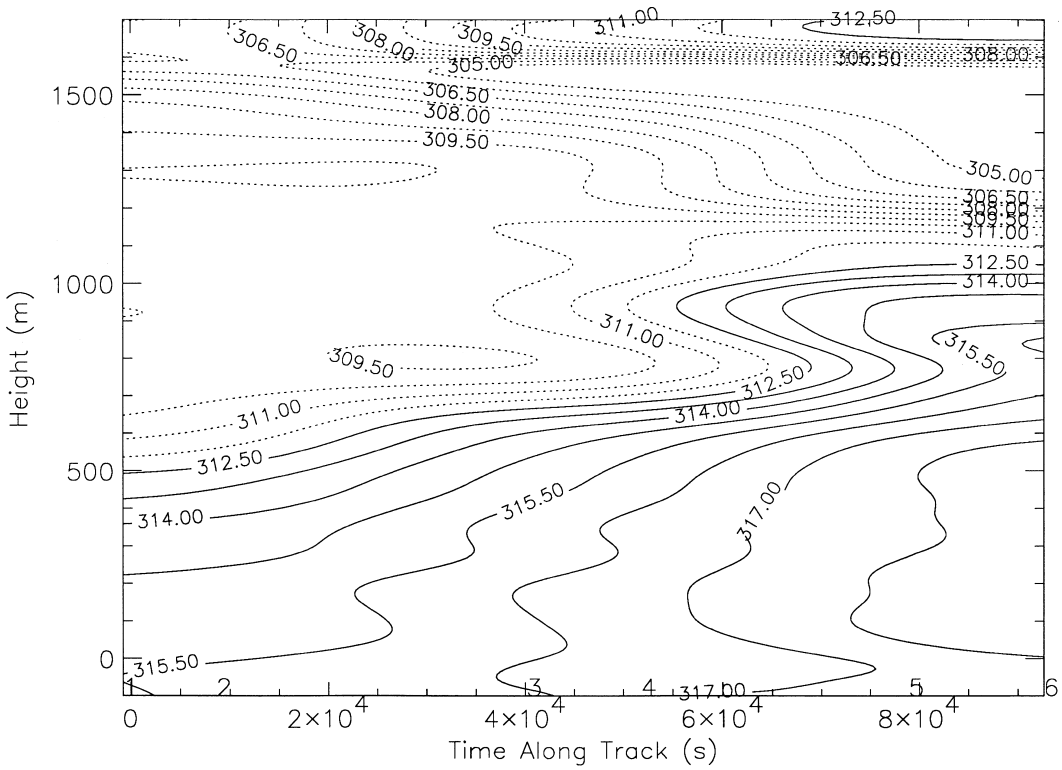

Fig. 3. The variation of equivalent potential temperature (K) in the lower atmosphere during the 1st Lagrangian experiment measured by the MRF C-130.

with accumulation mode concentrations of 50 cm^{-3} and there was very little change between the MBL and lower free troposphere. By the end of the 3rd flight though, this had increased to 200 cm^{-3}. In contrast, variations in the lower free troposphere were only small. Thus, by the end of the experiment there was a relatively sharp gradient in accumulation mode aerosol concentrations across the inversion. The double layer structure of the MBL had little effect on the accumulation mode concentrations that seemed to be well mixed throughout the depth of the MBL. However, the mean volume radius of the accumulation mode particles did vary in the vertical. The largest particles are found in the SML and the smallest in the free troposphere. Intermediate size particles are found in the cloud layer.

A large majority of the increase in accumulation mode aerosol concentrations can be explained by the increase in surface wind speed. This not only helped to enhance mechanical mixing within the MBL but also has the potential to increase salt particle production at the sea surface due to breaking waves. It is commonly agreed that once the wind speed exceeds 8 m s^{-1} salt particle production increases sharply (Woodcock, 1953; O'Dowd and Smith, 1993). During the 2nd flight (during daylight hours), "white capping" at the surface was widely observed. A time scale analysis carried out by Hoell et al. (2000) estimate that the changing wind conditions during the 26-h period of the experiment could contribute an extra accumulation mode concentration of 108 cm^{-3}, which is the same order of magnitude as the observed 150 cm^{-3} concentration increase. Table 2 summarises the mean aerosol and wind characteristics measured during the aircraft box patterns in the various layers of the lower atmosphere.

Fig. 8 shows the dry, aerosol size spectrum at the surface measured by the ship, on either side of the balloon release. This has a marked bimodal shape and the Aitken mode (0.01 μm to 0.1 μm

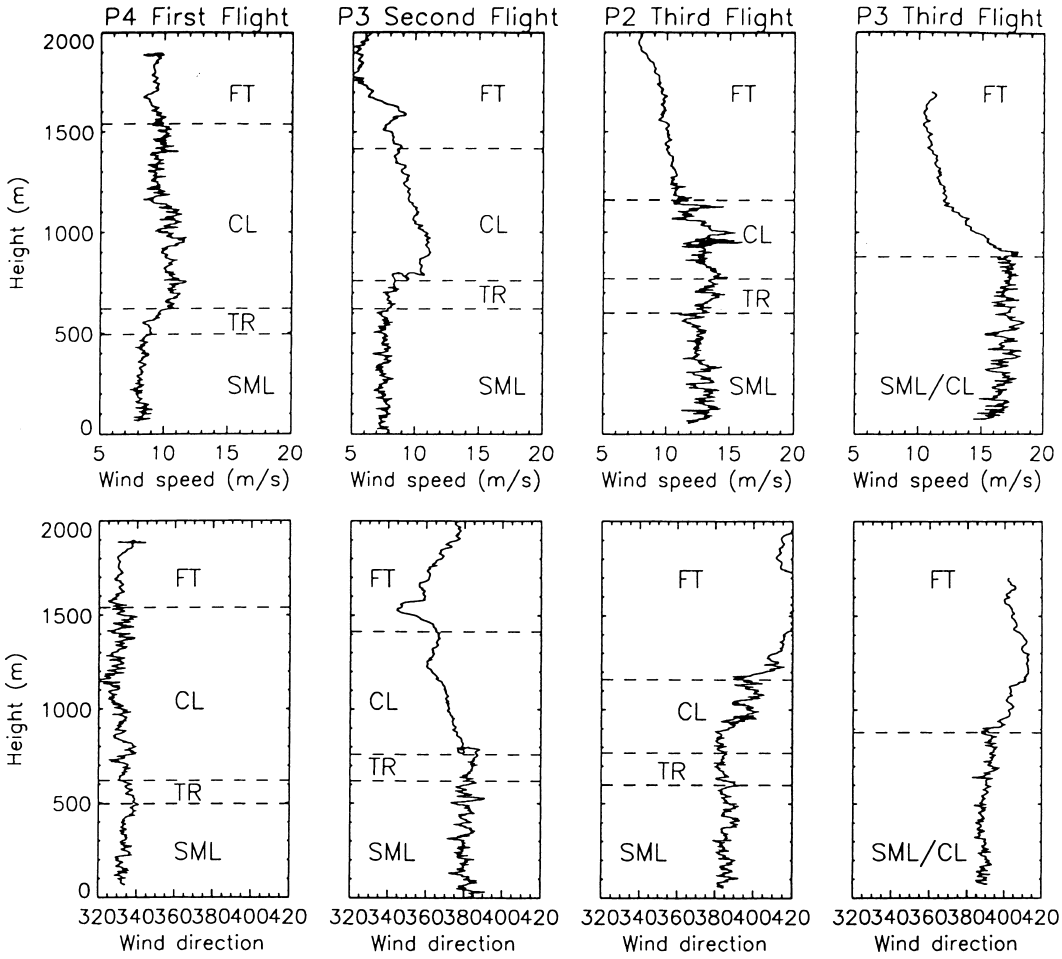

Fig. 4. Same as Fig. 2 except showing wind speed (top row), and wind direction (bottom row). For wind directions east of north 360 has been added to allow a continuous line to be drawn.

diameter) concentrations were at least an order of magnitude larger than the accumulation mode. The Aitken mode modal diameter was around 0.03 μm while the modal diameter of the accumulation mode was slightly bigger than 0.2 μm. During the balloon release the total CN (>3 nm) concentration was found to be $920 \pm 100\ \mathrm{cm}^{-3}$ and the aerosol >12 nm concentration was measured as $800 \pm 92\ \mathrm{cm}^{-3}$. As can be seen from Fig. 8 there was some variation in the shape of the aerosol size spectrum on relatively short time scales. So, even though the air was relatively clean there was some inhomogeneity within the air mass.

The fact that the Aitken mode and accumulation mode are separated by an identifiable trough in the size spectrum is indicative that the aerosol is being, or has been in the recent past, processed by clouds. The diameter of the concentration minimum is the smallest particle size that is being activated into cloud droplets (Hoppel et al., 1986). These are growing in size, either through aqueous phase chemical reactions or droplet coalescence, to enhance the accumulation mode part of the size spectra when the cloud droplets evaporate below cloud. There was very little cloud during the experiment so it is thought that most of the aerosol cloud processing occurred prior to the experiment when the air parcel was in the northern

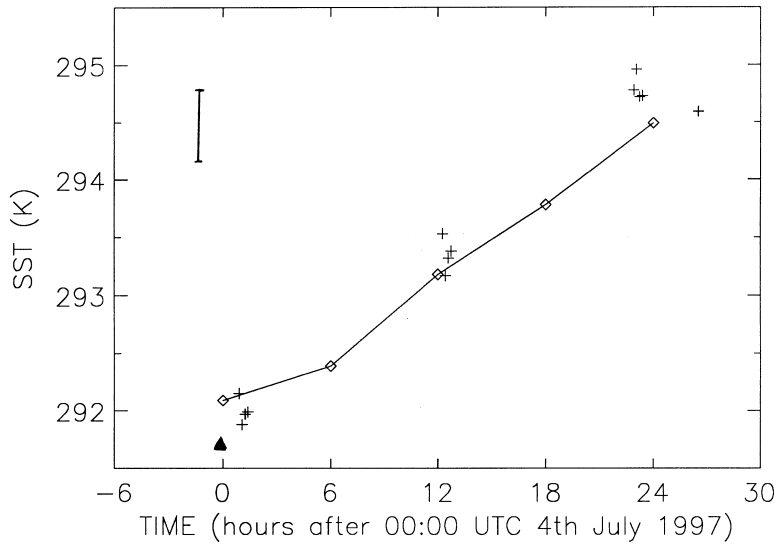

Fig. 5. The MRF C-130 measured sea surface temperature (crosses) and ECMWF analysed values (joined diamonds) along the track of the balloon in the 1st Lagrangian experiment. The solid triangle indicates the SST measured by the ship at balloon release. The error bar shows the accuracy of the aircraft measurements.

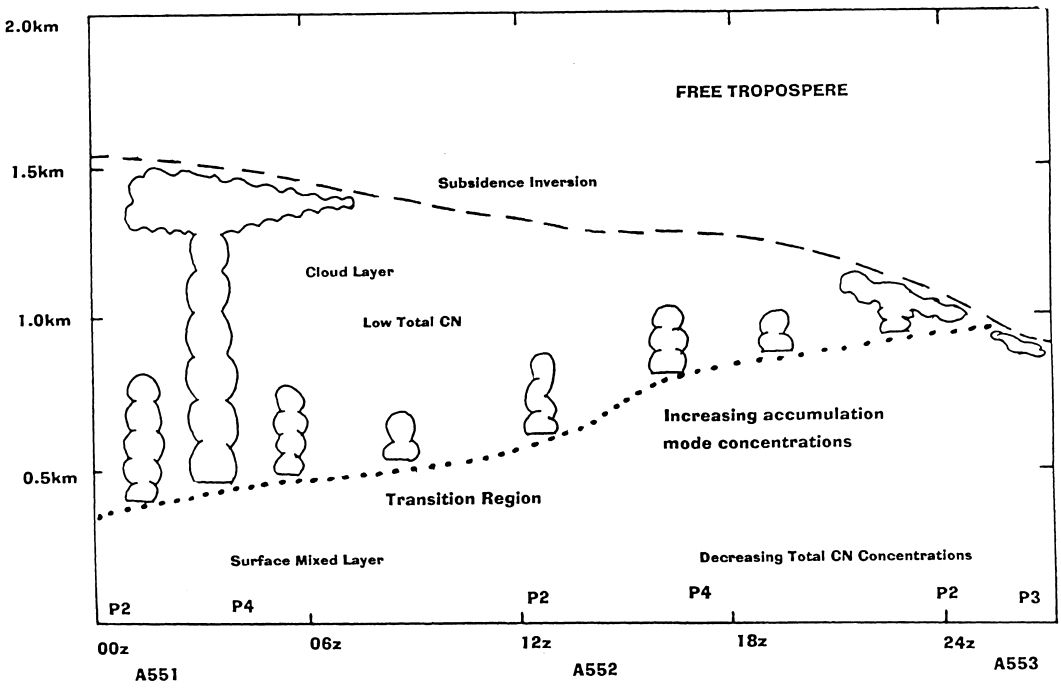

Fig. 6. A schematic diagram of the boundary layer, cloud and aerosol evolution during the 1st Lagrangian experiment.

Table 2. *A summary of the mean accumulation mode (N — 0.1 to 3.0 μm diameter) aerosol concentrations, mean total CN (>3 nm) concentrations, mean wind speed, mean wind direction and mean CCN concentrations at 0.2% supersaturation around the box patterns flown in each flight in each of the layers in the MBL and lower free troposphere*

Layer	Time (h)	Height (m)	N (cm^{-3})	Total CN (cm^{-3})	Wind speed ($m\ s^{-1}$)	Wind direction (deg)	CCN 0.2% (cm^{-3})
				1st flight			
SML	1.0	150	75	1245	7.8	336	35
		(5)	(25)	(375)	(1.2)	(5)	
bottom	1.7	510	95	1180	7.9	337	40
of CL		(3)	(30)	(425)	(0.9)	(7)	
top of	2.5	1040	85	1020	7.8	342	30
CL		(3)	(20)	(230)	(1.2)	(8)	
				2nd flight			
SML	12.4	33	115	1100	8.9	006	105
		(8)	(30)	(205)	(0.7)	(5)	
top of	13.2	338	120	1040	9.0	008	125
SML		(18)	(30)	(230)	(0.9)	(7)	
CL	13.8	1095	115	685	7.8	010	110
		(14)	(20)	(95)	(1.5)	(8)	
FT	14.5	2009	80	665	6.2	025	140
		(14)	(15)	(35)	(1.2)	(8)	
CL	15.3	1101	115	660	9.1	007	120
		(11)	(20)	(75)	(1.5)	(8)	
FT	16.1	2020	85	630	7.4	030	130
		(11)	(15)	(30)	(1.0)	(10)	
				3rd flight			
SML	23.0	95	160	880	14.2	026	155
		(4)	(25)	(100)	(1.0)	(4)	
SML	23.6	437	160	820	14.2	030	135
		(4)	(25)	(70)	(0.8)	(4)	
CL	24.4	743	155	725	14.5	029	180
		(3)	(30)	(75)	(1.1)	(5)	
top of	25.1	912	130	575	14.3	033	—
CL		(7)	(40)	(105)	(1.0)	(6)	
FT	25.8	1245	25	375	9.6	046	85
		(3)	(10)	(295)	(1.3)	(7)	
SML	26.5	132	155	725	15.0	021	210
		(5)	(30)	(45)	(0.7)	(4)	

The time indicates the time elapsed since the balloon was released from the ship. Before averaging, the values of N and total CN were filtered to remove penetrations of ship plumes and instrument artifacts caused by cloud penetrations. Numbers in brackets are variations around base pattern.

part of the anticyclone, where the cloud was more extensive in the MBL.

The total CN concentrations were dominated by the Aitken mode. So, although the accumulation mode aerosol concentrations showed a large increase during the experiment, the total CN measured in the SML was found to decrease in concentration from around $1000\ cm^{-3}$ to

Fig. 7. Same as Fig. 2 except showing total CN (>3 nm) concentrations (top row), accumulation mode (>0.1 μm and <3.0 μm) concentrations (second row) and mean volume diameter of accumulation mode aerosol concentrations (third row). Missing data segments are due to cloud penetrations that adversely effect the aerosol measurements due to droplet shattering on the instrument inlets.

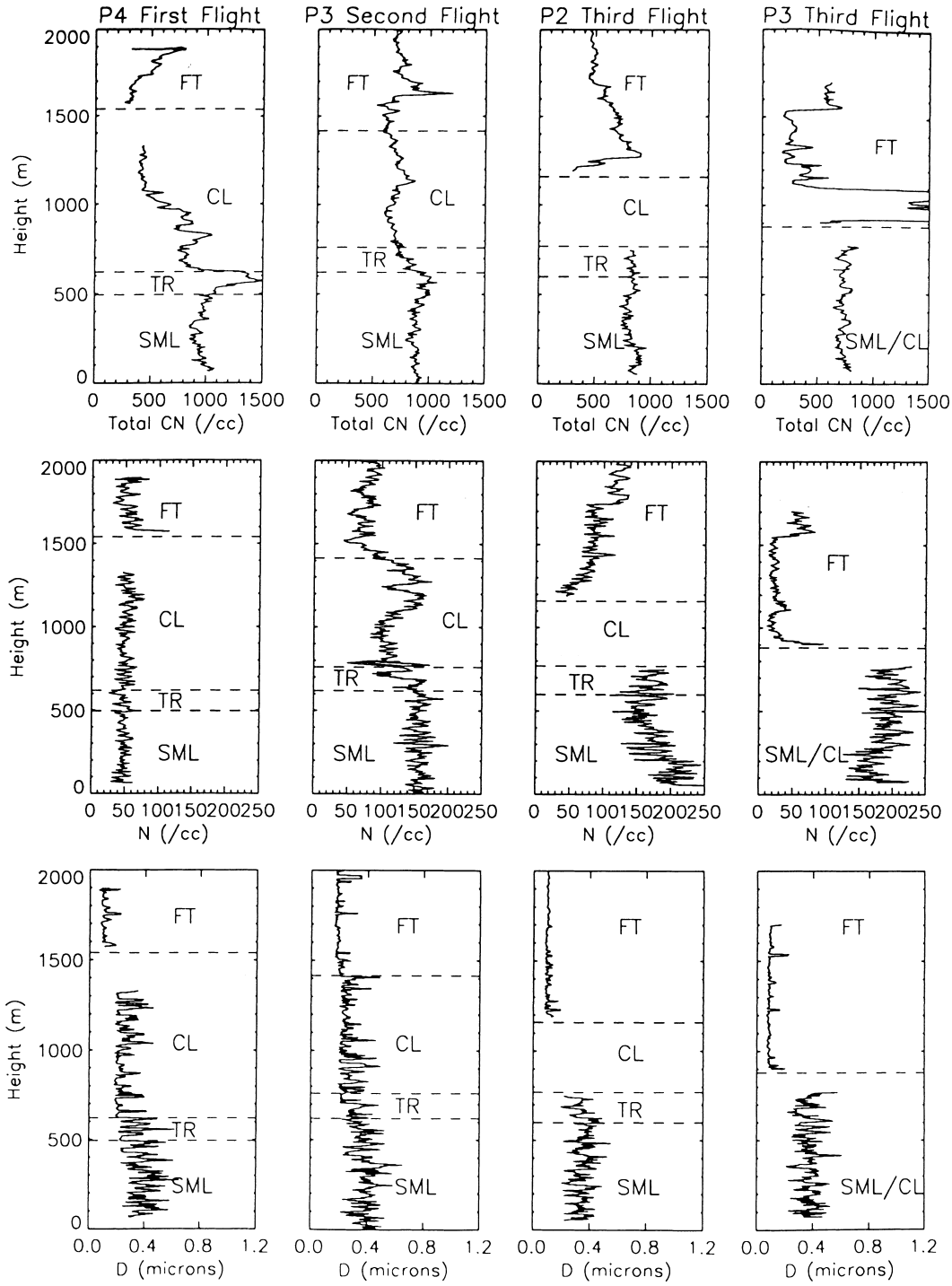
P4 First Flight
P3 Second Flight
P2 Third Flight
P3 Third Flight
Height (m)
2000
1500
1000
500
0
FT
CL
TR
SML
SML/CL
0 500 1000 1500
Total CN (/cc)
0 50 100150200250
N (/cc)
0.0 0.4 0.8 1.2
D (microns)

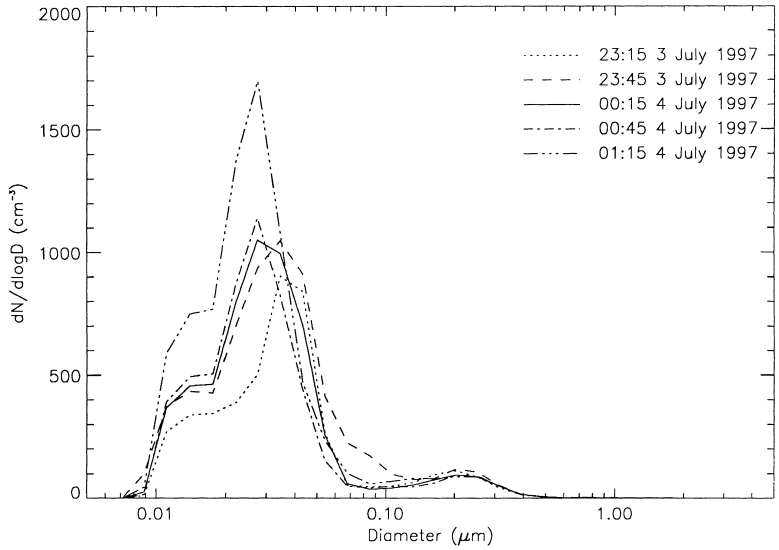

Fig. 8. The variation of the aerosol size spectra measured by the R/V *Vodyanitskiy* an hour either side of the release of the constant height "smart" balloons at the start of the 1st Lagrangian experiment. The aerosol was dried to a RH of 50%. All times are in GMT.

750 cm^{-3}. This can be seen in the aircraft profiles shown in Fig. 7. Also, in contrast to the accumulation mode aerosol, the multiple layering of the MBL had a pronounced effect on the total CN concentrations. The CL showed much greater variations in total CN concentrations and there were several hundred fewer particles in the CL compared to the SML. However, as the SML got deeper during the course of the experiment the vertical profiles of total CN concentration show far less variation.

The total CN concentrations in the lower free troposphere are around 500 cm^{-3} but there is some variation during the flights. In the 3rd flight, there is a marked change in the characteristics of the total CN above the MBL in profile P3. Just above the subsidence inversion base and the top of the stratocumulus, a layer of high aerosol concentrations is found over a depth of 200 m. The peak concentrations are around 2670 cm^{-3} (off the edge of Fig. 7). We are confident this was not an instrument artifact as the layer was flown through on a couple of occasions and its characteristics were similar each time. Differential horizontal advection of aerosol maybe the cause, but as the MBL air parcel was considered to be embedded in a large maritime air mass it is difficult to understand where a pollution layer would have come from. New particle nucleation in the upper free troposphere (Raes, 1995) which had subsided is similarly unlikely, as the high aerosol concentration layer is associated with a relatively high θ_e and RH. The layer may be similar to that observed by Hegg et al. (1990) and Clarke et al. (1998) during ACE-1 where it was found that nucleation was occurring in the outflow regions from cumuli, although the measurements presented here were made during the night. It is possible that some of the cumuli in the MBL had overshot the top of the MBL and detrained into the inversion layer. This would help explain the higher RH and θ_e values that were in effect diluted MBL air.

The majority of the increase in the accumulation mode concentrations occurs in the size range 0.1 μm to 0.3 μm diameter. This can be seen in the size spectra shown in Fig. 9. Here a comparison of the evolution of the aerosol size spectra in the SML, CL and lower free troposphere is shown. Each size spectrum plotted is the average along one run of a box pattern in the indicated layer. This is also borne out in Fig. 10 which shows measurements of the accumulation mode spectra from the CVI in aerosol mode underneath cloud in the SML for each of the 3 flights. In the last

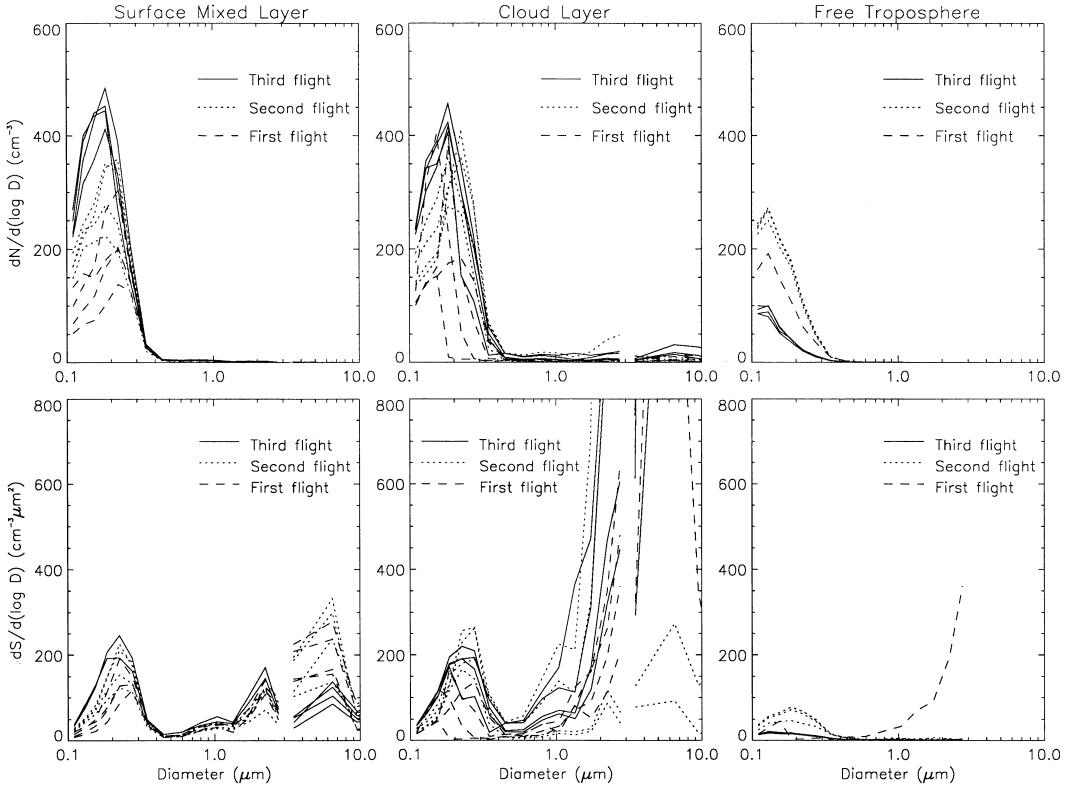

Fig. 9. The variation of accumulation mode (>0.1 μm and <3.0 μm) and coarse mode (>3.0 mm) aerosol size spectra measured with the MRF C-130 PCASP and FSSP respectively during the 3 flights in the 1st Lagrangian experiment in the surface mixed layer, cloud layer and lower free troposphere. The top row shows aerosol concentration and the bottom row, aerosol surface area. The aerosol was sampled at ambient RH.

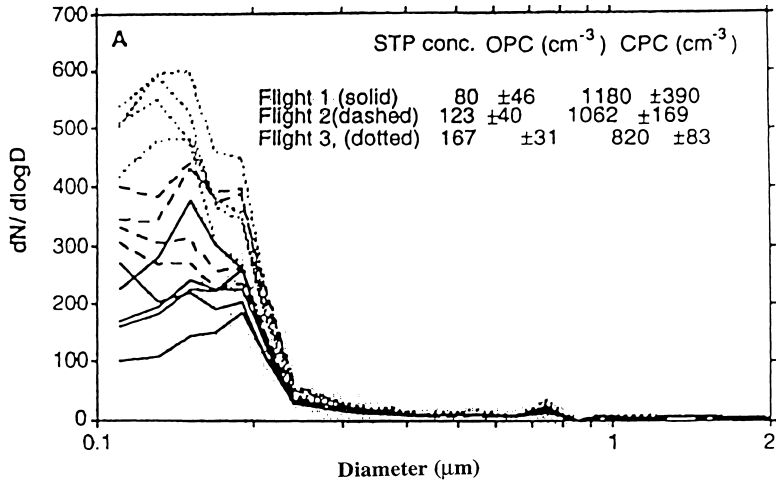

Fig. 10. The variation of accumulation mode (>0.1 μm and <3.0 μm) aerosol size spectra measured with the MRF C-130 CVI in aerosol mode during the 3 flights in the 1st Lagrangian experiment in the surface mixed layer.

flight there is evidence of a small increase in the larger particles (>0.4 μm diameter). The mode diameter in each of the spectra decreases as the concentrations get higher. O'Dowd and Smith (1993) found that in clean air masses, submicron sea salt aerosol concentrations showed a strong exponential increase with high wind speeds down to a dry particle diameter of 0.1 μm, which is very similar to what is being observed here. For the first time in these experiments it has been possible to follow the evolution of the aerosol characteristics under changing wind conditions, whereas in previous experiments only spot measurements of aerosol concentrations on different days under different wind conditions have been reported. There is a clear correlation here between increasing wind speed and increasing submicron aerosol concentrations. This can be seen in Fig. 11.

Fig. 12 shows time series of accumulation mode aerosol concentrations, wind speed, total CN concentrations and RH around boxes flown in the SML. The RH is relatively homogeneous in each of the flights, being about 70% in the 2nd and the 3rd flights and 80% in the first one. The large changes in accumulation mode aerosol concentrations between flights appear well correlated with the major changes in wind speed. In fact, the local variation of wind speed and accumulation mode aerosol concentration is also of some interest here. During the box patterns in the SML in the 2nd and 3rd flights, the wind speeds were high enough for significant white capping of the waves to be occurring. In the 1st flight, however the wind speed varied between 5 m s^{-1} and almost 10 m s^{-1} indicating perhaps that during the course of this box a significant increase in salt particle produc-

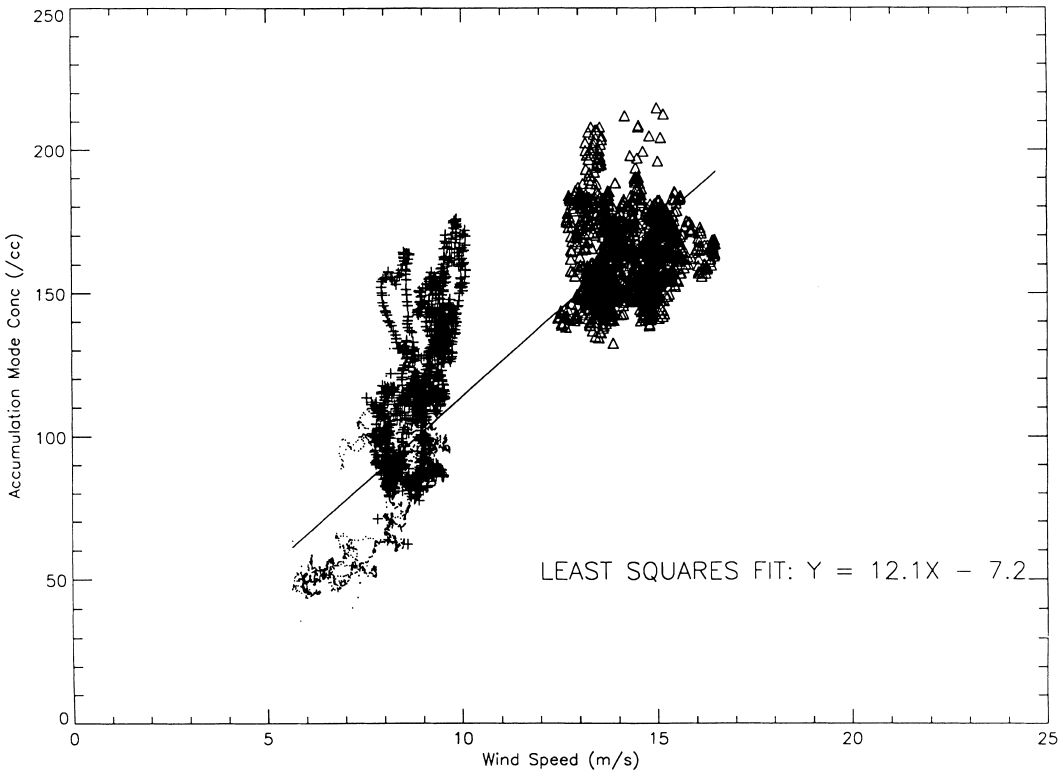

Fig. 11. A plot of wind speed against accumulation mode concentrations averaged over 20 s in box patterns flown near the bottom of the SML in each of the flights. Dots represent the 1st flight, crosses the 2nd flight and triangles the 3rd flight in the 1st Lagrangian experiment.

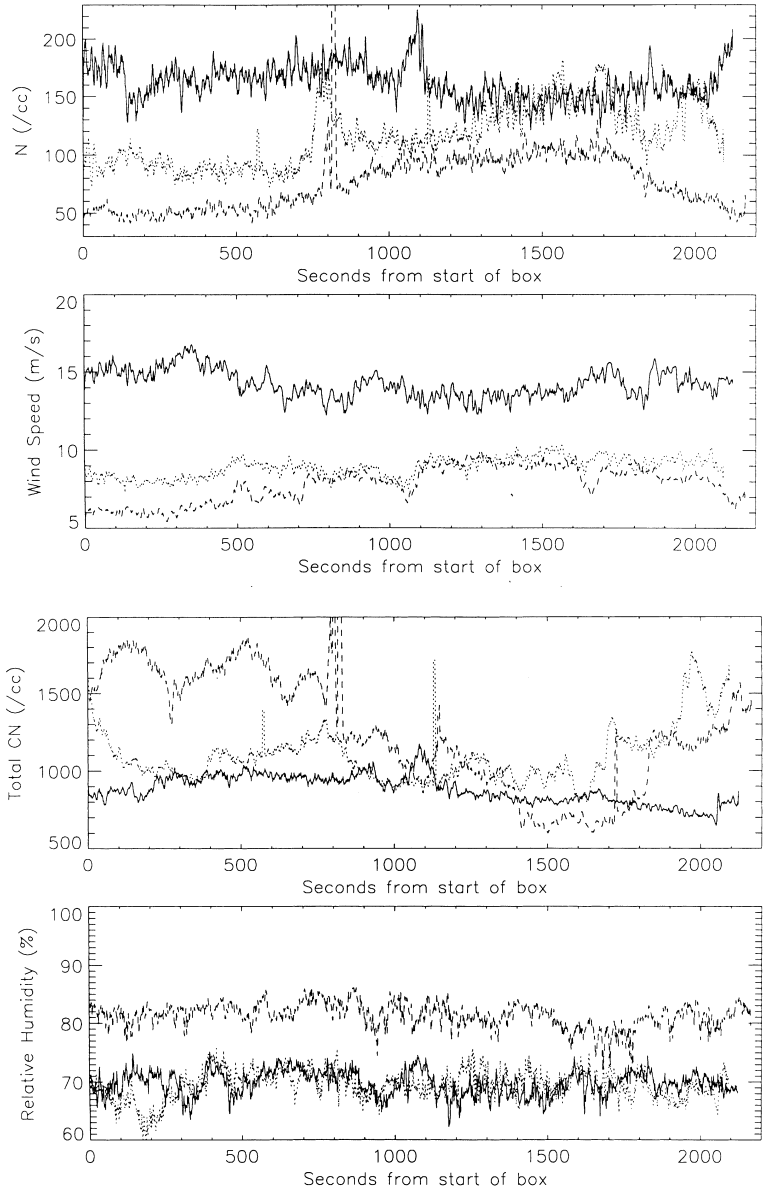

Fig. 12. Time series of accumulation mode (>0.1 μm and <3.0 μm) aerosol concentration (top diagram), wind speed (second diagram), total CN (>3 nm) concentrations (third diagram), and relative humidity (bottom diagram) around one of the MRF C-130 box patterns in the surface mixed layer during the 1st flight (dashed line), 2nd flight (dotted line), and 3rd flight (solid line) in the 1st Lagrangian experiment. The *x*-axis indicates the time from the start of the box pattern in seconds.

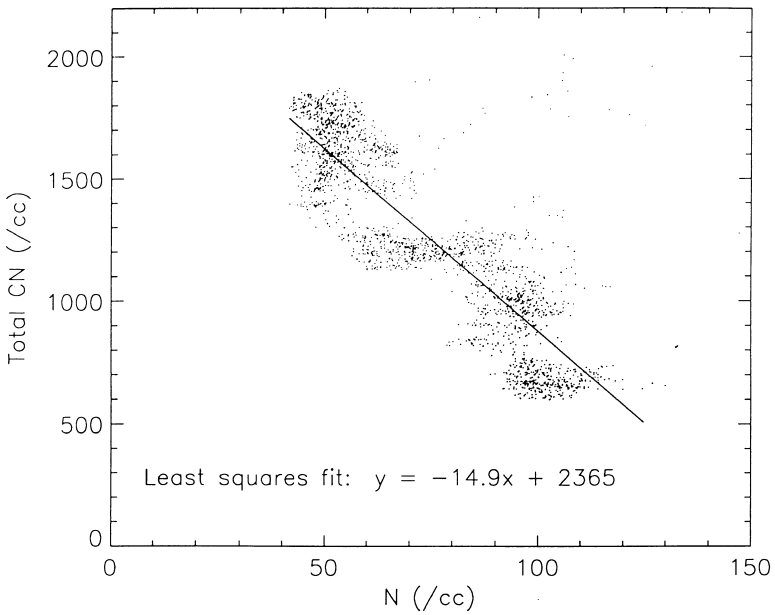

Fig. 13. A scatter plot of accumulation mode (>0.1 μm and <3.0 μm) aerosol concentration and total CN (>3 nm) concentration measured around one of the MRF C-130 box patterns in the surface mixed layer of the 1st flight in the 1st Lagrangian experiment.

tion would be initiated. There is certainly an increase in accumulation mode aerosol concentrations from less than 50 cm^{-3} to over 100 cm^{-3} during this run, which is in phase with the change in wind speed. The increase in salt particle surface area that this produces (see Fig. 9) has the potential to disrupt or modify the processes which were in pseudo equilibrium before the wind speed started to increase. This may help to explain why the total CN concentrations during this box are anti-correlated to the wind speed and accumulation mode aerosol concentrations. The total CN concentrations decrease from over 1700 cm^{-3} to 600 cm^{-3} in this time.

Fig. 13 shows a scatter plot of accumulation mode aerosol concentrations and total CN concentrations in the box pattern in the SML in the 1st flight. The anti-correlation between these parameters is very marked. It is difficult from the observations alone to determine what processes are occurring here. Further analysis and comparison with simulations from process models is required but we hypothesize that the increased aerosol surface area produced by the source of salt particles is enhancing the coagulation of accumulation mode and Aitken mode particles. Therefore as the accumulation mode aerosol particles increase in concentration due to the increasing wind speed, they are sweeping out more Aitken mode particles and as a result the total CN concentrations are decreasing. The anti-correlation of these 2 parameters is not as noticeable at other times in the flight. This should not be unexpected. The onset of significant salt particle production will have a major disruptive effect on the balance of the different aerosol processes occurring in the MBL. Once a continuous supply of salt particles has begun then a new process balance will be achieved.

It should be noted here that during the box in the 1st flight (800 s from the start of the box) the aircraft flew through a plume from a ship in the busy shipping lanes off the coast of Portugal. At this stage, the plume was very narrow (i.e., the penetration of the plume was close to the ship) and the peak concentration was several thousand

particles cm^{-3}. During the 2nd flight a broader plume, at a similar number of seconds from the start of the box was penetrated. Here the peak concentration was only 70 cm^{-3} above background levels due to the plume being diluted with distance downstream from the ship. A weaker plume still was also observed on the 3rd flight about 1100 s from the start of the box. These observations give us a great deal of confidence that the aircraft was following the same parcel of air on each flight.

6. Evolution of the cloud microphysics in the MBL

The increase in the accumulation mode concentrations observed in this experiment has a marked effect on the cloud condensation nuclei (CCN) concentrations in the MBL. Fig. 14 shows CCN supersaturation spectra measured with a thermal gradient diffusion chamber in the SML in each flight. The 2nd and 3rd flights have significantly higher CCN concentrations than the first one. Larger supersaturations tend to activate smaller aerosol particles. Therefore, the change in gradient that is observed in the supersaturation spectra with time indicates that higher concentrations of small accumulation mode particles were being produced.

Typically in this sort of MBL the maximum water supersaturation that would be achieved near cloud base would be ~0.3% (Martin et al., 1994). From these spectra, this supersaturation would produce droplet concentrations of approximately 50 cm^{-3} in the 1st flight whereas in the last 2 flights it would produce droplet concentrations above 150 cm^{-3}. This change in the CCN characteristics is evidenced in the change in the cloud microphysics. Fig. 15 show profiles of droplet concentrations, measured by an FSSP, and accumulation mode aerosol concentrations measured in the first and last flight of the experiment. In addition, Fig. 16 shows droplet spectra averaged over 30 m of cloud at the top of the MBL for the same profiles. When the air in the MBL is very clean at the start of the experiment, the clouds had droplet concentrations of 60 cm^{-3} whereas at the end of the experiment the cloud droplet concentrations had doubled to 120 cm^{-3}. Measurements from the CVI of the droplet residual particle spectra also indicate that droplet concentrations in the stratocumulus in the 3rd flight were more than 120 cm^{-3}. These droplet concentrations combined with the measured supersaturation spectra indicate that the maximum supersaturation in the cloud in the 1st flight was around 0.4% while in the last flight it was 0.18%. This indicates that

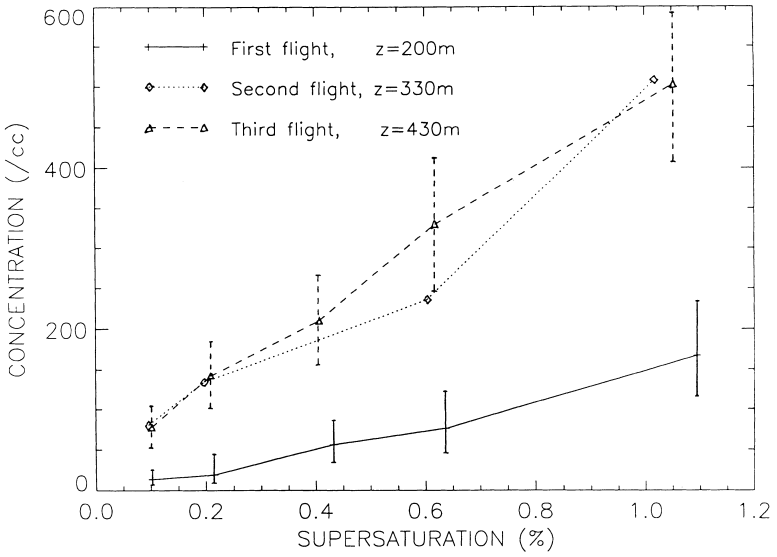

Fig. 14. CCN supersaturation spectra measured in the surface mixed layer in each of the 3 flights of the MRF C-130 in the 1st Lagrangian experiment.

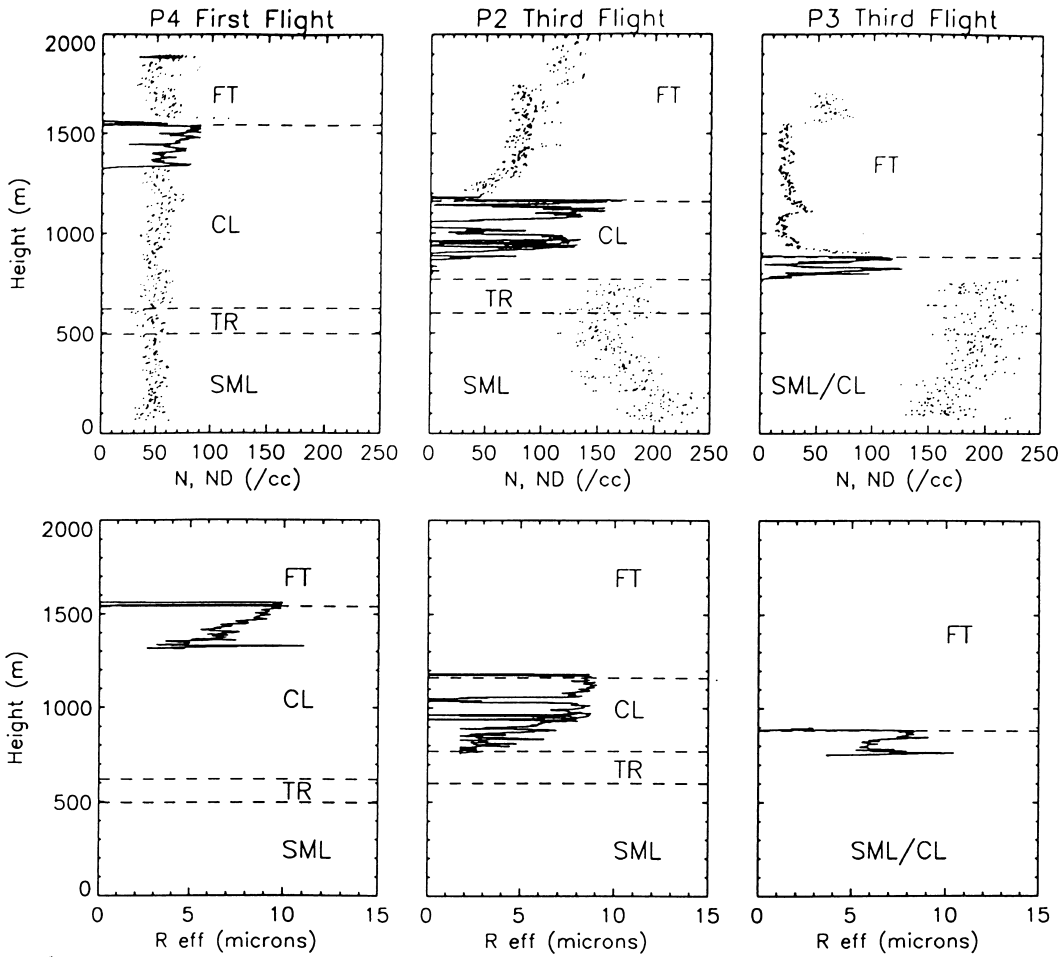

Fig. 15. Same as Fig. 2 except showing accumulation mode (>0.1 μm and <3.0 μm) aerosol concentrations (N, dotted line) and cloud droplet concentrations (ND, solid line) (top row), and cloud droplet effective radius (bottom row).

there was either much weaker overturning occurring in the later part of the experiment or the maximum supersaturation was being suppressed by the increased activation of larger numbers of aerosol particles into water droplets.

In the 1st flight all of the accumulation mode aerosol particles are being activated as can be seen by the 1:1 ratio of these parameters in Fig. 15. However, in the 3rd flight although the cloud droplet concentration increases it does not match the quadrupling of the accumulation mode concentration. This could be for one of 2 reasons. Either some of the new sub-micron sea salt particles are not big enough to be activated at the reduced maximum supersaturations or entrainment of dry, clean free tropospheric air into the cloud top is suppressing the cloud droplet concentrations. There is evidence that both of these processes are occurring. This change in the aerosol and cloud microphysics has a marked effect on the shape of the cloud droplet size spectrum. In the 1st flight, the size spectrum has a classical clean air mass shape with a prominent mode at around 18 μm. In the final flight the modal diameter is decreased to less than 10 μm and is beginning to take on more of the appearance of a

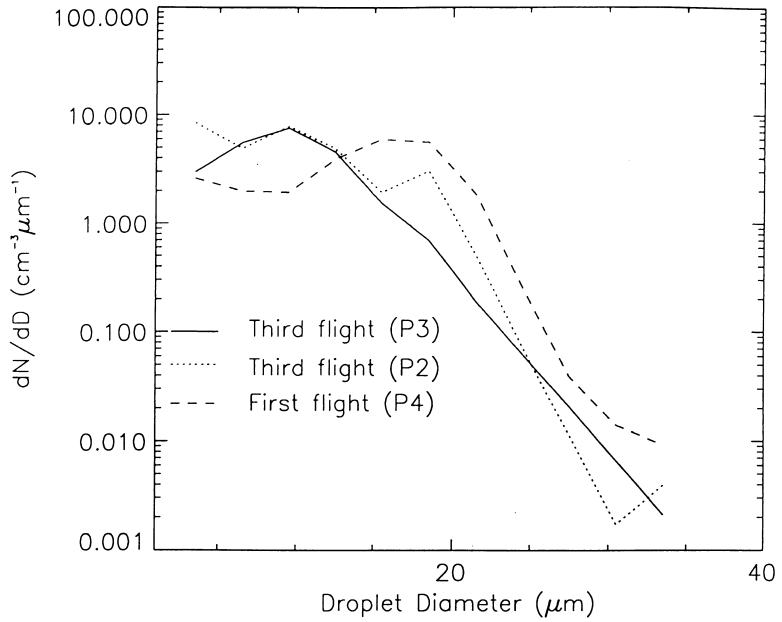

Fig. 16. A comparison of cloud droplet size spectra during MRF C-130 cloud penetrations near the top of the boundary layer in each of the 3 flights in the 1st Lagrangian experiment.

slightly dirty cloud with more of a uni-modal appearance. This change in shape of the spectra reduces the maximum effective radius (R_e — the ratio of the third moment of the spectra to the second moment (Martin et al., 1994)) measured at cloud top during the experiment; as seen in Fig. 15. R_e in the 1st flight has a maximum value of 10 μm whereas in the last flight it is reduced to 8 μm. As there is little change in the liquid water path of these clouds the changes in droplet size and number concentration will have a significant effect on the radiative characteristics of the cloud. The clouds will have a progressively higher albedo during the experiment.

7. The chemical characteristics of the aerosol and trace gases

7.1. Aerosol chemistry

The ion chromatography analysis of the filters collected on the aircraft show that the soluble fine mode (< 1.4 μm diameter) aerosol has a large component of ammonium sulphate. Table 3 shows the molar mixing ratios of the soluble fine mode aerosol. The ratio of ammonium to sulphate mixing ratio measurements is generally a little greater than 2 indicative of ammonium sulphate being present in the parcel of air. There is a small tendency for the ammonium sulphate to increase during the course of the experiment. The next largest component of the soluble fine mode aerosol is sea salt and this is found to increase significantly as would be expected due to the observed increase in wind speed.

Sea salt dominates the soluble coarse mode (> 1.4 μm diameter) aerosol. Table 4 presents the molar mixing ratios of the soluble coarse mode aerosol. While the absolute concentrations of the sea salt species in the coarse mode are only about one third of the actual values because of inlet losses, the relative amounts between samples are valid indicators of the change in sea salt fractional mass. In both the fine mode and coarse mode aerosol results there seems to be very little consistent variation of either ammonium sulphate or sea particle concentrations with height in the MBL. The mixing between the SML and the CL appears

Table 3. *Concentrations (ppt molar mixing ratios) of soluble fine mode (<1.4 μm diameter) aerosol composition measured during the 1st Lagrangian experiment using filters exposed on the MRF C-130 aircraft in specific layers of the boundary layer (SML — surface mixed layer, and CL — cloud layer) and free troposphere (FT). The numbers in brackets refer to the uncertainty in the analysis*

Layer	Na^+	NH_4^+	K^+	Mg^{++}	Ca^{++}	MSA	Cl^-	NO_3^-	SO_4^{2-}
					1st flight				
SML	61	187	<40	<20	<60	<5	76	34	60
	(63)	(16)	(40)	(18)	(52)	(4)	(46)	(31)	(18)
CL	702	153	<40	28	<50	<3	656	36	72
	(55)	(13)	(35)	(16)	(46)	(3)	(50)	(27)	(16)
FT	<30	115	<20	<10	<25	<3	<20	12	39
	(28)	(9)	(18)	(8)	(23)	(2)	(20)	(14)	(8)
SML	95	211	21	<10	<70	<3	159	18	104
	(39)	(16)	(14)	(12)	(67)	(3)	(29)	(14)	(7)
					2nd flight				
top of	64	316	<30	21	25	<5	162	46	127
SML	(66)	(24)	(24)	(20)	(113)	(5)	(48)	(24)	(10)
CL	267	242	99	84	355	<5	213	50	125
	(58)	(19)	(21)	(18)	(99)	(4)	(42)	(21)	(9)
FT	<70	145	<30	<20	<120	<5	<50	46	51
	(63)	(13)	(23)	(19)	(107)	(5)	(46)	(23)	(10)
					3rd flight				
SML	101	259	<50	29	105	<5	194	33	111
	(82)	(19)	(46)	(17)	(41)	(4)	(29)	(32)	(15)
top of	196	207	<40	25	<30	<3	265	48	106
SML	(64)	(15)	(36)	(13)	(32)	(3)	(24)	(25)	(12)
CL	191	212	<40	31	<30	<3	272	19	104
	(67)	(16)	(37)	(14)	(33)	(3)	(25)	(26)	(12)
top of	200	113	<30	22	<30	<3	227	<20	62
CL	(45)	(9)	(25)	(9)	(23)	(2)	(20)	(18)	(8)
FT	<90	67	<50	<20	57	<5	30	<40	29
	(87)	(8)	(48)	(18)	(44)	(4)	(31)	(34)	(16)

to be occurring on shorter time scales than the lifetime of the aerosol particles and so a well-mixed MBL in terms of the aerosol composition is being maintained. It is speculated that the cumulus clouds are playing a role here. These will locally rapidly mix SML air which is dragged up into the CL, and then the broader downdraughts associated with the cumulus clouds will enhance the entrainment of CL air back into the SML.

Filter samples collected from the CVI probe in aerosol mode have also been analysed using an ion chromatograph technique. Table 5 shows the mass ($\mu g\, m^{-3}$) of aerosol for individual soluble species. This shows that the sea salt sulphate mass increases by 50% from the 1st flight to the 3rd flight in the SML, consistent with the physical aerosol measurements made by the aircraft. However, both sets of filters also suggest that the non-sea salt sulphate increases between 10% (CVI filters) and 50% (filter packs) during the course of the experiment. This indicates that sulphate mass must be being produced locally. The small concentrations of SO_2 available in the MBL are enough for either aqueous phase chemistry in the cloud droplets to produce sulphate on existing CCN, thereby improving their CCN characteristics or by the direct deposition of SO_2 onto the aerosol particles below cloud base. The first of these processes would tend to enhance the bimodal characteristics of the aerosol spectrum by increasing mass in the accumulation mode, whereas the latter would tend to fill in the trough between the Aitken mode and the accumulation mode. As there is very little observational evidence that the

Table 4. *Concentrations (ppt molar mixing ratios) of soluble large (>1.4 μm diameter) aerosol composition measured during the 1st Lagrangian experiment using filters exposed on the MRF C-130 aircraft in specific layers of the boundary layer (SML — surface mixed layer, and CL — cloud layer) and free troposphere (FT). The numbers in brackets refer to the uncertainty in the analysis*

Layer	Na^+	NH_4^+	K^+	Mg^{++}	Ca^{++}	MSA	Cl^-	NO_3^-	SO_4^{2-}
					1st flight				
SML	442	<10	<10	46	<20	2.0	347	23	30
	(7)	(7)	(7)	(7)	(21)	(3)	(25)	(7)	(2)
CL	201	<10	<10	22	178	<3	159	24	9
	(8)	(8)	(8)	(8)	(23)	(3)	(27)	(8)	(2)
FT	389	<10	<10	49	35	2.3	268	69	47
	(6)	(6)	(6)	(6)	(18)	(2)	(22)	(6)	(3)
					2nd flight				
SML	530	<5	9	65	22	4.5	364	47	37
	(21)	(5)	(12)	(5)	(7)	(2)	(23)	(3)	(2)
top of	712	<10	20	66	37	3.2	552	74	48
SML	(35)	(9)	(20)	(9)	(11)	(4)	(36)	(5)	(4)
CL	1418	<10	<20	96	15	<3	651	74	51
	(31)	(8)	(18)	(8)	(10)	(3)	(41)	(5)	(3)
FT	47	<10	<20	<10	<10	<4	49	<5	<3
	(33)	(9)	(19)	(9)	(10)	(3)	(10)	(5)	(3)
					3rd flight				
SML	806	<10	22	85	35	<3	668	<7	53
	(22)	(7)	(6)	(5)	(10)	(3)	(43)	(7)	(7)
top of	410	<5	11	44	7	2.4	335	<5	25
SML	(17)	(5)	(4)	(3)	(8)	(2)	(22)	(5)	(5)
CL	871	10	33	91	33	<3	690	7	61
	(18)	(6)	(5)	(6)	(8)	(2)	(44)	(6)	(6)
top of	358	<5	12	43	22	1.8	259	<4	24
CL	(12)	(4)	(3)	(3)	(5)	(2)	(17)	(4)	(4)
FT	<30	<10	<10	5	<10	<3	<15	<8	<7
	(24)	(7)	(6)	(3)	(10)	(3)	(15)	(7)	(7)

Table 5. *Mass ($\mu g\ m^{-3}$) of aerosol for individual soluble species determined from the filters sampling air collected by the CVI inlet set up in aerosol mode, compared with the mass calculated from the PCASP connected to the CVI probe using a density of 2 g cm^{-3}*

OPC mass	Total ionic species	Na	Cl	Sea salt SO_4	Non-sea salt SO_4	NO_3	NH_4
				1st flight			
10.6	10.5	2.3	4.2	0.62	0.60	0.26	0.13
(±1.9)	(±0.3)	(±0.2)	(±0.1)	(±0.03)	(±0.02)	(±0.01)	(±0.02)
				3rd flight			
15	14.4	3.5	6.5	0.93	0.67	1.74	0.37
(±2)	(±0.3)	(±0.2)	(±0.2)	(±0.03)	(±0.02)	(±0.07)	(±0.04)

trough is being filled in, it is likely that much of the extra non-sea salt sulphate mass is coming from cloud processing. The time scale analysis carried out by Hoell et al. (2000) also reinforces this view as they estimate that under the conditions of this experiment aqueous phase chemistry will produce sulphate mass an order of magnitude faster than simple condensation will.

7.2. *Trace gas chemistry*

SO_2 concentrations were determined by the aircraft using filter samples exposed in each of the layers in the MBL and the lower free troposphere. In general the SO_2 levels were low and close to the detection limit of the technique used and the concentrations measured on the ship were all below the 100 ppt detection limit of their instrument. In the SML the concentrations varied between 17 ($\pm$8) and 40 ($\pm$18) ppt and in the CL between $<$10 ($\pm$4) and 24 ($\pm$7) ppt suggesting that perhaps there is some loss of SO_2 through cloud processing. However, this difference may not be significant in view of the large analytical uncertainties associated with the low SO_2 values observed, which were comparable to results obtained from remote, unpolluted locations, and were probably sustained by the oxidation of DMS.

Radon and carbon monoxide were both measured by the R/V *Vodyanitskiy* and the MRF C-130 aircraft, respectively. Both were observed to be at very low levels, close to or below the detection limits of the instruments as would be expected in a clean maritime air mass. Ozone and H_2O_2 are both important oxidants for the production of sulphate through aqueous phase reactions depending on the water acidity. Both gases were measured, although, due to instrument problems, H_2O_2 was only sampled on the 2nd flight. Included in Fig. 2 were profiles of ozone concentration from each of the flights. These showed a significant amount of vertical variability that mirrored the layered structure of the MBL. The lowest values were observed in the SML at around 30 ($\pm$4) ppb. This compared well with the ship measurement of 27 ppb. In the CL, they rose to approximately 40 ($\pm$4) ppb with an increase across the TR. In the lower free troposphere, the concentrations were generally more than 50 ($\pm$5) ppb. Very little change in the concentration was observed with time, which suggests that the ozone was in a dynamic equilibrium. The lower concentrations in the SML are likely to be a result of dry deposition to the sea surface and the chemical destruction of ozone in the high RH (McFadyen et al., 2000). Entrainment of ozone from the CL and lower free troposphere will then act as a source of ozone to continually top up the concentrations in the SML.

H_2O_2 concentration measurements on the aircraft showed that it rose almost linearly in the SML from 0.9 ppb to 1.3 ppb. This is not surprising as the sea surface is a strong sink of H_2O_2. Through the TR and CL, H_2O_2 is almost constant and acts as a source of H_2O_2 for the SML through slow entrainment mechanisms. The organic peroxide concentration decreases throughout the MBL from 0.5 ppb at the surface to 0.1 ppb at the top of the MBL.

During the 1st Lagrangian experiment, 9 bottle samples from the different layers in the MBL and lower free troposphere were collected for analysis of NMHCs. Over 90 species of NMHC we estimated from the samples. However, as would be expected in a clean air mass the NMHC mixing ratios are relatively small and close to background levels.

8. Summary and conclusions

The 1st ACE-2 Lagrangian experiment followed the evolution of the MBL structure, aerosol and cloud microphysical characteristics in a clean maritime air mass over a period of 30 h. Significant changes occurred to the parcel of air being followed. Although the MBL started very clean, the accumulation mode aerosol concentrations quadrupled during the period of the experiment so that the MBL ended up with relatively high concentrations of CCN for a maritime air mass, while the total CN concentrations decreased by 25%. The challenge has been, and will be, to try to explain this. Aerosol modeling studies of this case are only just beginning, so the main aim of this paper has been to collate all the measurements made and to put forward the best description of the evolution of the air mass as we can. From this, hypotheses are suggested for the important processes causing the air mass evolution, which

can be tested by process models in the future. The ultimate aim of this work will be to quantitatively identify and understand these processes so that realistic aerosol parametrisations can be developed for global climate models to improve our estimates of the direct and indirect radiative forcing of aerosols.

The main results of the ACE-2 1st Lagrangian experiment were as follows.

(a) The MBL was characterised by 2 layers — a SML and a CL in which scattered cumuli spread out into well-broken stratocumulus under a subsidence inversion.

(b) Significant subsidence ($0.45\ cm\ s^{-1}$) in the free troposphere decreased the depth of the MBL from 1500 m to 900 m.

(c) The surface wind speed increased from $8\ m\ s^{-1}$ to $16\ m\ s^{-1}$. This combined with increased surface fluxes due to the air passing over a warmer SST deepened the SML from 500 m to 900 m where the top of the SML merged with the subsidence inversion.

(d) The aerosol size spectrum had a marked bi-modal shape and the Aitken mode was found to dominate the aerosol number concentration.

(e) The accumulation mode aerosol concentrations increased from $50\ cm^{-3}$ to $200\ cm^{-3}$ throughout the depth of the MBL. Most of the number concentration increase in the accumulation mode was in the size ranges 0.1 μm to 0.3 μm diameter.

(f) The total CN concentrations decreased from $1000\ cm^{-3}$ to $750\ cm^{-3}$ in the SML but were half these values in the CL.

(g) The increase in accumulation mode aerosol mass in the MBL was primarily attributable to a 50% increase in sea salt mass.

(h) Non-sea salt sulphate mass in the MBL increased between 10 and 50%.

(i) CCN concentrations in the MBL with 0.3% maximum water supersaturation increased from $50\ cm^{-3}$ to $150\ cm^{-3}$.

(j) Cloud droplet concentrations increased from $60\ cm^{-3}$ to $120\ cm^{-3}$.

The main changes to the accumulation mode and total CN concentrations can be explained by the significant increase in wind speed observed in the MBL. This dramatically increased the source of salt particles at the sea surface through breaking waves and this increased aerosol surface area may have enhanced coagulation of Aitken mode and accumulation mode particles, which lead to an overall decrease in the total CN concentrations. However, there is also other evidence that suggests that interstitial scavenging of Aitken mode particles by cloud droplets and entrainment of air from the lower free troposphere into the MBL maybe playing a role in decreasing the total CN concentrations. The measured increase in non-sea salt sulphate mass in the MBL may be moving aerosol mass from the Aitken mode into the accumulation mode (thereby contributing to the accumulation mode aerosol concentration increase) by condensation of SO_2 onto the aerosol, but it is more likely that the non-sea salt sulphate mass production is arising through aqueous phase reactions within cloud and thus will result in larger accumulation mode aerosol which will have better CCN characteristics. Due to the large change in CCN characteristics in the MBL the cloud microphysics also changed significantly, with over a doubling of the cloud droplet concentration and a decrease in the droplet effective radius. This had a marked change on the radiative transfer characteristics of the cloud.

8.1. Hypotheses

More work in comparing the data analysis and simulations of process modeling is required before a full interpretation of the processes can be made. In order to facilitate this hypotheses have been formulated for process models to test and validate. They are as follows.

- Salt particle production at the sea surface accounts for the majority of the accumulation mode concentration increase in the MBL (at sizes <0.3 μm diameter).
- Aqueous phase reactions in cloud oxidize dissolved SO_2 into sulphate thereby increasing the sulphate mass in the MBL.
- The increased salt particle surface area enhances condensation of SO_2 produced by DMS emissions from the sea surface thereby increasing the sulphate mass in the MBL.
- The increased salt particle surface area enhances coagulation of accumulation and Aitken

mode particles thereby decreasing total CN concentrations.

- Condensation of sulphate onto existing aerosol particles moves mass/concentration from the Aitken mode to the accumulation mode.
- In-cloud scavenging causes a decrease in total CN (the scavenging is mainly from the Aitken mode particles).
- The decrease in Aitken mode concentrations is primarily due to dilution with entrained free tropospheric air.

The 1st Lagrangian experiment of ACE-2 was carried out in a relatively clean maritime air mass and it has acted as a very good comparison with the other 2 Lagrangians that were in polluted, continental air masses (Osborne et al, 2000; Wood et al., 2000). It has provided a framework for studying the important aerosol processes occurring over the sea. For the first time, a parcel of air has been followed for a significant length of time in a marine environment where the synoptic conditions were changing substantially such that the disturbance of the delicate balance of processes controlling the aerosol size spectrum by a major source of new aerosol could be investigated in detail. The database collected here should form a good foundation for future validation and improvement of large-scale numerical model parametrisation of salt particle production at the sea surface.

9. Acknowledgements

This research is a contribution to the International Global Atmospheric Chemistry (IGAC) Core project of the International Geosphere-Biosphere Programme (IGBP) and is part of the IGAC Aerosol Characterisation Experiments (ACE). It has been supported by the European Union under contract ENV4-CT95-0032. Further support was obtained from the UK DETR, NERC, the German Max Planck Society, Joint Research Centre and other national agencies in Sweden, Germany, USA, and Canada. Support is also gratefully acknowledged from the Spanish Meteorological Service, ECMWF, and UK Meteorological Office for the forecasts for the ACE-2 area and the trajectory analysis that made accurate prediction of the timing of the Lagrangian experiment possible. Thanks are due to the many collaborators, support staff, students, ship crew, and RAF aircrew who could not all be mentioned in the list of contributors.

REFERENCES

Albrecht, B. A., Bretherton, C. S., Johnson, D. W., Schubert, W. H. and Frisch, A. S. 1995. The Atlantic Stratocumulus Transition Experiment — ASTEX. *Bull. Amer. Met. Soc.* **76**, 6, 889–904.

Andreae, M. O. and Crutzen, P. J. 1997. Atmospheric aerosols: biogeochemical sources and role in atmospheric chemistry. *Science* **276**, 1052–1058.

Andreae, M. O., Berresheim, H., Andreae, T. W., Kritz, M. A., Bates, T. S. and Merril, J. T. 1988. Vertical distribution of dimethylsulfide, sulfur dioxide, aerosol ions and radon over the north east Pacific Ocean. *J. Atmos. Chem.* **6**, 149–173.

Bates, T. S., Kapustin, V. N., Quinn, P. K., Covert, D. S., Coffman, D. J., Mari, C., Durkee, P. A., De Bruyn, W. J. and Saltzman, E. S. 1998. Processes controlling the distribution of aerosol particles in the lower marine boundary layer during the first aerosol characterisation experiment. *J. Geophys. Res.* **103**, 16,369–16,383.

Bates, T. S., Quinn, P. K., Covert, D. S., Coffman, D. J., Johnson, J. E. and Weidensohler, A. 2000. Aerosol physical properties and controlling processes in the lower marine boundary layer: a comparison of submicron data from ACE-1 and ACE-2. *Tellus* **52B**, 258–272.

Baumgardner, D. 1983. An analysis and comparison of five water droplet measuring instruments. *J. Appl. Meteor.* **22**, 891–910.

Blanchard, D. C. and Woodcock, A. H. 1957. Bubble formation and modification in the sea and its meteorological significance. *Tellus* **9**, 145–158.

Chin, M. and Jacob, D. J. 1996. Anthropogenic and natural contributions to tropospheric sulfate: a global model analysis. *J. Geophys. Res.* **101**, 18,691–18,699.

Chin, M., Jacob, D. J., Gardner, G. M., Foreman, N. S., Spiro, P. A. and Savoie, D. L. 1996. A global three dimensional model of tropospheric sulfate. *J. Geophys. Res.* **101**, 18,667–18,690.

Clarke, A.D., Uehara, T. and Porter, J. N. 1996. Lagrangian evolution of an aerosol column during the Atlantic stratocumulus transition experiment. *J. Geophys. Res.* **101**, 4351–4362.

Clarke, A. D., Varner, J. L., Eisele, F., Mauldin, R. L., Tanner, D. and Litchy, M. 1998. Particle production in the remote marine atmosphere: cloud outflow and subsidence during ACE-1. *J. Geophys. Res.* **103**, D13, 16,397–16,409.

Dore, A., Johnson, D. W., Osborne, S., Choularton, T., Bower, K., Andreae, M. O. and Bandy, B. 2000. The evolution of boundary layer aerosol particles due to in-cloud chemical reactions during the second Lagrangian experiment of ACE-2. *Tellus* **52B**, 452–463.

Draxler, R. R. and Hess, G. D. 1997. *Description of hysplit 4 modeling*. Technical Memorandum ERL ARL-224, NOAA.

Fiengold, G., Kreidenweiss, S. M., Stevens, B. and Cotton, W. R. 1996. Numerical simulations of stratocumulus processing of cloud condensation nuclei through collision coalescence. *J. Geophys. Res.* **101**, 21,391–21,402.

Fitzgerald, J. W., Marti, J. J., Hoppel, W. A., Frick, G. M. and Gelbard, F. 1998. A one dimensional sectional model to simulate multicomponent aerosol dynamics in the marine boundary layer (2). Model application. *J. Geophys. Res.* **103**, 16,103–16,117.

Hegg, D. A., Radke, L. F. and Hobbs, P. V. 1990. Particle production associated with marine clouds. *J. Geophys. Res.* **95**, 13,917–13,926.

Hoell, C., O'Dowd, C., Johnson, D. W., Osborne, S. R. and Wood, R. 2000. A time scale analysis of aerosol evolution in polluted and clean Lagrangian case studies. *Tellus* **52B**, 423–438.

Hoppel, W. A., Frick, G. M. and Larson, R. E. 1986. Effect of non-precipitating cloud on the aerosol size distribution in the marine boundary layer. *Geophys. Res. Lett.* **13**, 125–128.

Huebert, B. J., Pszenny, A. and Blomquist, B. 1996. The ASTEX/MAGE Experiment. *J. Geophys. Res.* **101**, D2, 4319–4329.

Johnson, D. W., Osborne, S., Wood, R., Suhre, K., Johnson, R., Businger, S., Quinn, P. K., Wiedensohler, A., Durkee, P. A., Russell, L. M., Andreae, M. O., O'Dowd, C., Noone, K., Bandy, B., Rudolph, J. and Rapsomanikis, S. 2000. An overview of the Lagrangian experiments undertaken during the North Atlantic regional aerosol characterisation experiment. *Tellus* **52B**, 290–320.

Johnson, R., Businger, S. and Baerman, A. 2000. Lagrangian air mass tracking with smart balloons during ACE-2. *Tellus* **52B**, 321–334.

Martin, G. M., Johnson, D. W. and Spice, A. 1994. The measurement and parametrisation of effective radius of droplets in warm stratocumulus clouds. *J. Atmos. Sci.* **51**, 1823–1842.

Martin, G. M., Johnson, D. W., Rogers, D. P., Jonas, P. R., Minnis, P. and Hegg, D. 1995. Observations of the interactions between cumulus clouds and warm stratocumulus in the marine boundary layer during ASTEX. *J. Atmos. Sci.* **52**, 16, 2902–2922.

McFadyen, G. G., Cape, J. N., Flynn, M., Bandy, B. J. and Wood, R. 2000. Entrainment and photochemistry of ozone in the marine boundary layer during ACE-2 HILLCLOUD. *Tellus* **B**, in press.

Nicholls, S., Leighton, J. and Barker, R. 1990. A new fast response instrument for measuring total water content from aircraft. *J. Atmos. Oceanic Technol.* **7**, 706–718.

O'Dowd, C. D. and Smith, M. H. 1993. Physiochemical properties of aerosols over the Northeast Atlantic: evidence for wind speed related submicron sea salt aerosol production. *J. Geophys. Res.* **98**, 1137–1149.

O'Dowd, C. D., Smith, M. H., Consterdine, I. E. and Lowe, J. A. 1997. Marine aerosol, sea-salt and the marine sulphur cycle: a short review. *Atmos. Res.* **31**, 73–80.

Osborne, S. R., Johnson, D. W., Wood, R., Bandy, B. J., Andreae, M. O., O'Dowd, C., Glantz, P., Noone, K., Rudolf, J., Bates, T. and Quinn, P. 2000. Observations of the evolution of the aerosol, cloud and boundary layer dynamic and thermodynamic characteristics during the second Lagrangian experiment of ACE-2. *Tellus* **52B**, 375–400.

Penkett, S. A., Bandy, B. J., Reeves, C. E., McKenna, D. and Hignett, P. 1995. Measurements of peroxides in the atmosphere and their relevance to the understanding of global tropospheric chemistry. *Faraday Discussions* **100**, 155–174.

Quinn, P. K., Bates, T. S., Coffman, D. J., Miller, T. L. and Johnson, J. E. 2000. A comparison of aerosol chemical and optical properties from the first and second aerosol characterisation experiments. *Tellus* **52B**, 239–257.

Raes, F. 1995. Entrainment of free tropospheric aerosols as a regulating mechanism for cloud condensation nuclei in the remote marine boundary layer. *J. Geophys. Res.* **100**, 2893–2903.

Raes, F., Bates, T. S., McGovern, F. M. and Van Liedekerke, M. 2000. The second aerosol characterisation experiment (ACE-2): general overview and main results. *Tellus* **52B**, 111–126.

Rogers, D. P., Johnson, D. W. and Friehe, C. A. 1995. The stable internal boundary layer over the coastal sea (I). Airborne measurements of the mean and turbulence structure. *J. Atmos. Sci.* **52**, 667–683.

Sollazzo, M. J., Russell, L. M., Percival, D., Osborne, S., Wood, R. and Johnson, D. W. 2000. Entrainment rates calculated from ACE-2 aircraft measurements. *Tellus* **52B**, 335–347.

Talbot, R. W, Andreae, M. O., Berresheim, H., Artaxo, P., Garstang, M. Harris, R. C., Beecher, K. M. and Li, S. M. 1990. Aerosol chemistry during the wet season in central Amazonia: the influence of long range transport. *J. Geophys. Res.* **95**, 16,955–16,969.

Taylor, K. E. and Penner, J. E. 1994. Responses of the climate system to atmospheric aerosols and greenhouse gases. *Nature* **369**, 734–737.

Van Dingenen, R., Raes, F., Putaud, J.-P., Virkkula, A.

and Mangoni, M. 1999. Processes determining the relationship between aerosol number and non-sea-salt sulfate mass concentration in the clean and perturbed marine boundary layer. *J. Geophys. Res.* **104**, 8027–8038.

Wood, R., Johnson, D. W., Osborne, S. R., Bandy, B. J., Andreae, M. O., O'Dowd, C., Glantz, P. and Noone, K. J. 2000. Boundary layer, aerosol and chemical evolution during the third Lagrangian experiment of ACE-2. *Tellus* **52B**, 401–422.

Woodcock, A. H. 1953. Salt nuclei in marine air as a function of altitude and wind force. *J. Met.* **10**, 362.